$RuX(CO)(NO)L_2$ and $Ru(CO)(NO)L_2^+$: Ru(0) or Ru(II) or In Between?

Masamichi Ogasawara, Dejian Huang, William E. Streib, John C. Huffman, Nuria Gallego-Planas, Feliu Maseras, Odile Eisenstein,* and Kenneth G. Caulton*

Contribution from the Department of Chemistry and Molecular Structure Center, Indiana University, Bloomington, Indiana 47405-4001, and LSDSMS UMR 5636, Université de Montpellier 2, 34095 Montpellier Cedex 5, France

Received February 21, 1997[⊗]

Abstract: The synthesis of $RuCl(CO)(NO)L_2$ (L = P^tBu_2Me) and replacement of Cl^- by BF_4^-, CO, CH_3CN, H_2O, F^-, and H^- are reported. $NaBAr^F_4$ (Ar^F = 3,5-$(CF_3)_2C_6H_3$) removes halide to produce the four-coordinate 16-electron cation $Ru(NO)(CO)L_2^+$, shown by X-ray diffraction to have a nonplanar structure symptomatic of greater back bonding than isoelectronic $Ru(CO)_2L_2$. Variable-temperature ^1H NMR studies of the ^{t}Bu groups in $[Ru(NO)(CO)L_2](BAr^F_4)$ show a $\Delta G^‡$ (100 °C) for inversion through planar Ru of 19.1 kcal/mol. $Ru(\eta^1\text{-}BF_4)(CO)(NO)L_2$ is shown by X-ray diffraction to have a square-pyramidal structure with apical bent NO. The IR frequencies of NO and CO are analyzed to conclude that all five-coordinate species except $Ru(NO)(CO)_2L_2^+$ and $RuH(NO)(CO)L_2$ have bent nitrosyls; these last two have linear NO. $RuX(CO)(NO)(PH_3)_2^+$ (X = Cl^-, BF_4^-, H^-, no ligand, NCH, CO) was calculated with *ab initio* calculations at the Becke3LYP level. Depending on the nature of X, one minimum (square pyramid with bent NO) or two minima (square pyramid with bent NO and trigonal bipyramid with linear NO) have been located. The difference in energy between these two structures follows closely the NO vibrational frequency. While the frontier between bent and linear NO is indistinct, the results clearly show that π-donor ligands stabilize 16-electron unsaturated species.

Introduction

We recently established that, with sufficient steric protection via the bulky phosphine L, it is possible to make the otherwise transient and highly reactive 16-electron, zerovalent species $Ru(CO)_2L_2$ "persistent".[1] Isolation and characterization, including an X-ray diffraction structure determination, of $Ru(CO)_2(P^tBu_2Me)_2$ revealed it to be distorted tetrahedral, not planar like other four-coordinate Rh(I), Ir(I) Pd(II), and Pt(II) d^8 16-electron analogs.[2] We also studied its reactivity toward sterically unencumbered reactants,[1b] including measurements of enthalpy of binding of MeNC and PhCCPh and of oxidative addition of the C−H bond of PhCCH to $Ru(CO)_2L_2$, where L = P^tBu_2Me, P^iPr_3, and PCy_3.[3]

In extending this unusual new class of unsaturated Ru(0) compounds, we were interested in several questions: (1) possible modification of the $Ru(CO)_2L_2$ complex (after some trials of alternation of the phosphine L,[4] here we focus on the modification of dicarbonyl moiety) and (2) the energy difference between the observed tetrahedral ground state and a planar structure. Since the tetrahedral structure was explained as a result of electronic stabilization by deformation away from a planar structure, estimation of the energy difference between these seems important to understand the origin of this unusual structure. If the energy difference between the two isomers is *not* so large, the complex might show the fluxional process in solution as shown in Scheme 1. We sought to use the two *tert*-butyl groups of P^tBu_2Me as probes of any such inversion of Ru through a square planar transition state; Scheme 1 shows how the environments of ^{t}Bu(1) and ^{t}Bu(2) are reversed by such fluxionality if a molecule can be made where X ≠ Y. After some initial misadventures toward this goal,[5] we now report the synthesis and characterization of $Ru(CO)(NO)(P^tBu_2Me)_2^+$ and related complexes, including their solution behavior. This study also reveals the reactivity consequences of replacement of CO by NO^+ in otherwise analogous four-coordinate, species. Finally, a reactivity study of $Ru(CO)(NO)L_2^+$ with a variety of nucleophiles X has led to the characterization of the coordination geometry and NO bending in the resulting $RuX(CO)(NO)L_2^+$. This has led to the proposal that an either/or choice of linear (NO^+) or bent (NO^-) states does not adequately describe physical reality, and leads to the provocative idea that a continuum of formal oxidation states must be accepted. This extends, into the σ and π influence of a ligand X, the ideas of Enemark and Feltham.[6] Overviews of nitrosyl chemistry, including its bending,[7] are available.[8]

Scheme 1

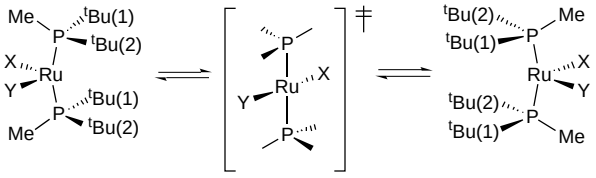

[⊗] Abstract published in *Advance ACS Abstracts,* September 1, 1997.

(1) (a) Ogasawara, M.; Macgregor, S. A.; Streib, W. E.; Folting, K.; Eisenstein, O.; Caulton, K. G. *J. Am. Chem. Soc.* **1995**, *117*, 8869. (b) Ogasawara, M.; Macgregor, S. A.; Streib, W. E.; Folting, K.; Eisenstein, O.; Caulton, K. G. *J. Am. Chem. Soc.* **1996**, *18*, 10189.

(2) Bennett, M. A.; Bruce, M. I.; Matheson, T. W. *Compr. Organomet. Chem.* **1982**, *4*, 691.

(3) Li, C.; Ogasawara, M.; Nolan, S. P.; Caulton, K. G. *Organometallics* **1996**, *16*, 4900.

(4) (a) Ogasawara, M.; Maseras, F.; Gallego-Planas, N.; Streib, W. E.; Eisenstein, O.; Caulton, K. G., *Inorg. Chem.* **1996**, *35*, 7468. (b) Ogasawara, M.; Maseras, F.; Gallego-Planas, N.; Kawamura, K.; Ito, K.; Toyota, K.; Streib, W. E.; Komiya, S.; Eisenstein, O.; Caulton, K. G. *Organometallics* **1997**, *16*, 1979.

(5) Although we have attempted to prepare $Ru(CO)(CNMe)(P^tBu_2Me)_2$[1b] and $Ru(CO)(CS)(P^tBu_2Me)_2$, in both cases, the complexes could not be made in isolable form. M. Ogasawara, unpublished observations.

(6) Enemark, J. H.; Feltham, R. C. *Coord. Chem. Rev.* **1974**, *13*, 339.

(7) Basolo, F. *Polyhedron* **1990**, *9*, 1503.

S0002-7863(97)00563-5 CCC: $14.00

Experimental Section

General. All manipulations were carried out with standard Schlenk and glovebox techniques under prepurified argon. Benzene, THF, and toluene were dried over sodium benzophenone ketyl, distilled, and stored in gas-tight solvent bulbs. Dichloromethane and acetonitrile were dried over CaH_2, distilled, and degassed by freeze−pump−thaw prior to use. Ethanol and methanol were degassed under vacuum and used without further purification. Benzene-d_6, toluene-d_8, dichloromethane-d_2, THF-d_8, diglyme-d_{14}, and 1,1,2,2-tetrachloroethane-d_2 were dried by appropriate methods and vacuum-distilled prior to use. *N*-Methyl-*N*-nitroso-*p*-toluenesulfonamide, $AgBF_4$, CsF, and $NaBH_4$ were purchased from Aldrich Chemical Co. and used without purification. $Na[B(C_6H_3\text{-}3,5\text{-}(CF_3)_2)]_4$($NaBAr^F_4$) was synthesized by a published method.[9] Gaseous reagents (H_2 and CO) were purchased from Air Products and used as received. $RuHCl(CO)(P^tBu_2Me)_2$ was synthesized as reported.[10] ^1H and ^{31}P NMR spectra were recorded on a Varian XL300 spectrometer (^1H, 300 MHz; ^{31}P, 122 MHz) or on a Varian INOVA 400 spectrometer (^1H, 400 MHz; ^{31}P, 161 MHz). ^{19}F NMR spectra were recorded on a Varian Gemini 300 spectrometer at 282 MHz. ^1H NMR chemical shifts are reported in ppm downfield of tetramethylsilane with use of residual solvent resonances as internal standards. ^{31}P NMR chemical shifts are relative to an external 85% H_3PO_4. ^{19}F chemical shifts are externally referenced to $CFCl_3$. Infrared spectra were recorded on a Nicolet 510P FT-IR spectrometer. Elemental analyses were performed on a Perkin-Elmer 2400 CHNS/O elemental analyzer at Indiana University.

$RuCl(CO)(NO)(P^tBu_2Me)_2$ (1). A suspension of $RuHCl(CO)(P^tBu_2Me)_2$ (2.00 g, 4.12 mmol) and *N*-methyl-*N*-nitroso-*p*-toluenesulfonamide (1.00 g, 4.67 mmol) in ethanol (70 mL) was placed in a Schlenk flask and refluxed for 2 h under argon. During this period, the suspension turned to a deep red, clear solution. After filtration, the solution was concentrated to *ca.* 35 mL under reduced pressure and cooled to −40 °C, yielding two crops of dark red crystals; yield 1.92 g (3.73 mmol, 91%). ^1H NMR (C_6D_6, 20 °C): δ 1.05 (vt, J_{HP} = 6.8 Hz, 18H, P−^{t}Bu), 1.17 (vt, J_{HP} = 6.8 Hz, 18H, P−^{t}Bu), 1.37 (vt, J_{HP} = 3.5 Hz, 6H, P−Me). $^{31}P\{^1H\}$ NMR (C_6D_6, 20 °C): δ 45.3 (s). IR: ν_{CO}(C_6D_6) = 1914 cm^{-1}, ν_{NO}(C_6D_6) = 1570 cm^{-1}. Anal. Calcd for $RuC_{19}H_{42}O_2ClNP_2$: C, 44.31; H, 8.22; N, 2.72. Found: C, 44.37; H, 7.94; N, 2.54.

$Ru(FBF_3)(CO)(NO)(P^tBu_2Me)_2$ (2). A mixture of $RuCl(CO)(NO)(P^tBu_2Me)_2$ (500 mg, 0.97 mmol) and $AgBF_4$ (185 mg, 0.95 mmol) in toluene (25 mL) was placed in a Schlenk flask and stirred at 50 °C for 10 min. After the gray precipitate was filtered away at this temperature, the filtrate was cooled to −40 °C to give two crops of orange crystals; yield 452 mg (0.80 mmol, 84%). ^1H NMR (CD_2Cl_2, 20 °C): δ 1.16 (vt, J_{HP} = 6.3 Hz, 18H, P−^{t}Bu), 1.21 (vt, J_{HP} = 6.3 Hz, 18H, P−^{t}Bu), 1.60 (vt, J_{HP} = 3.5 Hz, 6H, P−Me). $^{31}P\{^1H\}$ NMR (CD_2Cl_2, 20 °C): δ 56.2 (s). ^{19}F NMR (CD_2Cl_2, 20 °C): δ −160.7 (s). IR (CD_2Cl_2): ν_{CO} = 1917 cm^{-1}, ν_{NO} = 1572 cm^{-1}. Anal. Calcd for $RuC_{19}H_{42}O_2BF_4NP_2$: C, 40.29; H, 7.47; N, 2.47. Found: C, 40.64; H, 7.12; N, 2.74.

$[Ru(CO)(NO)(P^tBu_2Me)_2][B(C_6H_3\text{-}3,5\text{-}(CF_3)_2)_4]$ (3). (a) From $RuCl(CO)(NO)(P^tBu_2Me)_2$. A mixture of $RuCl(CO)(NO)(P^tBu_2Me)_2$ (100 mg, 0.19 mmol) and $NaBAr^F_4$ (175 mg, 0.20 mmol) was placed in a Schlenk flask and 5 mL of CH_2Cl_2 was added to the flask under argon. After a short period of homogeneity, gray-white precipitate formed. After removing the precipitate by filtration, the solution was concentrated to *ca.* 1 mL under reduced pressure and cooled to −40 °C, yielding red-orange crystals. Although X-ray single-crystal structure determination showed co-crystallization of dichloromethane (see text), prolonged evacuation of the crystals gives the solvent-free complex; yield 188 mg (0.14 mmol, 72%). ^1H NMR (CD_2Cl_2, 20 °C): δ 1.23 (vt, J_{HP} = 7.6 Hz, 18H, P−^{t}Bu), 1.31 (vt, J_{HP} = 7.6 Hz, 18H, P−^{t}Bu), 1.63 (vt, J_{HP} = 3.2 Hz, 6H, P−Me), 7.53 (br, 4H, *p*-$C_6H_3(CF_3)_2$), 7.69 (br, 8H, *o*-$C_6H_3(CF_3)_2$). $^{31}P\{^1H\}$ NMR (CD_2Cl_2, 20 °C): δ 59.6 (s). ^{19}F NMR (CD_2Cl_2, 20 °C): δ −61.5 (s). IR (CD_2Cl_2): ν_{CO} = 1966 cm^{-1}, ν_{NO} = 1709 cm^{-1}. Anal. Calcd for $RuC_{51}H_{54}O_2BF_{24}NP_2$: C, 45.62; H, 4.05; N, 1.04. Found: C, 45.62; H, 4.22; N, 1.30.

(b) From $Ru(FBF_3)(CO)(NO)(P^tBu_2Me)_2$. To a solution of $Ru(FBF_3)(CO)(NO)(P^tBu_2Me)_2$ (15 mg, 26 μmol) in CD_2Cl_2 (0.6 mL) was added $NaBAr^F_4$ (24 mg, 27 μmol). After the mixture was stirred for 15 min at room temperature, ^1H and ^{31}P NMR and IR spectra showed complete conversion of $Ru(FBF_3)(CO)(NO)(P^tBu_2Me)_2$ into $[Ru(CO)(NO)(P^tBu_2Me)_2][B(C_6H_3\text{-}3,5\text{-}(CF_3)_2)_4]$.

$[Ru(CO)_2(NO)(P^tBu_2Me)_2]BF_4$ (4). A THF solution of $Ru(FBF_3)(CO)(NO)(P^tBu_2Me)_2$ (100 mg, 0.18 mmol) was placed in a Schlenk flask and headspace was evacuated by a freeze−pump−thaw cycle. Introduction of CO (1 atm) to the flask at 0 °C gave immediate precipitation of pink-purple microcrystals. After the supernatant was removed, the complex was dried under a slow stream of CO. One of the two CO ligands is very labile, and satisfactory elemental analysis could not be obtained; all spectral data are recorded under 1 atm of CO. Yield: 84 mg (0.14 mmol, 80%). ^1H NMR (CD_2Cl_2, 20 °C): δ 1.41 (vt, J_{HP} = 7.7 Hz, 36H, P−^{t}Bu), 1.78 (vt, J_{HP} = 3.0 Hz, 6H, P−Me). $^{31}P\{^1H\}$ NMR (CD_2Cl_2, 20 °C): δ 59.8 (s). IR (CD_2Cl_2): ν_{CO} = 2045 and 1995 cm^{-1}, ν_{NO} = 1738 cm^{-1}.

$Ru(FBF_3)(CO)(NO)(P^tBu_2Me)_2$ + CH_3CN. In an NMR tube fitted with a rubber septum, $Ru(FBF_3)(CO)(NO)(P^tBu_2Me)_2$ (15 mg, 0.027 mmol) was dissolved in CD_2Cl_2 (0.5 mL). To this was added acetonitrile (1.5, μL, 0.029 mmol) by means of syringe. Although ^1H and ^{31}P NMR and IR spectra showed complete consumption of $Ru(FBF_3)(CO)(NO)(P^tBu_2Me)_2$, the product could not be isolated because of a rapid exchange between coordinating and free acetonitrile (see text for detail). ^1H NMR (CD_2Cl_2, 20 °C): δ 1.19 (vt, J_{HP} = 6.3 Hz, 18H, P−^{t}Bu), 1.22 (vt, J_{HP} = 7.2 Hz, 18H, P−^{t}Bu), 1.60 (vt, J_{HP} = 3.2 Hz, 6H, P−Me), 2.75 (br, 3H, CH_3CN). $^{31}P\{^1H\}$ NMR (CD_2Cl_2, 20 °C): δ 50.2 (s). IR (CD_2Cl_2): ν_{CO} = 1952 cm^{-1}, ν_{NO} = 1597 cm^{-1}; ν_{CN} = 2303 cm^{-1}.

$[Ru(CO)_2(NO)(P^tBu_2Me)_2][BAr^F_4]$. A solution of $[Ru(CO)(NO)(P^tBu_2Me)_2][BAr^F_4]$ (50 mg, 0.037 mmol) in CH_2Cl_2 was placed in a Schlenk flask, and the headspace was evacuated by a freeze−pump−thaw cycle. Introduction of CO (1 atm) to the flask at room temperature changed the solution color from orange to pale pink. The solvent was evaporated and the residue was dissolved in CH_2Cl_2, which was layered with pentane. Pale gray crystals formed in 18 h. Yield: 44 mg (87%). ^1H NMR ($CDCl_3$, 20 °C): δ 1.35 (vt, J_{HP} = 7.8 Hz, 36H, P^{t}Bu), 1.67 (vt, J_{HP} = 3 Hz, 6H, PMe). 7.50 (s, 4H, *p*-aryl), 7.70 (s, 8H, *o*-aryl). $^{31}P\{^1H\}$ NMR ($CDCl_3$, 20 °C). δ 57.4 (s). IR ($CDCl_3$): ν_{CO} = 2047, 1996 cm^{-1}, ν_{NO} = 1738 cm^{-1}. Anal. Calcd for $RuC_{52}H_{54}O_3BF_{24}NP_2$: C, 45.46; H, 3.97; N, 1.02. Found: C, 45.34; H, 3.90; N, 1.53.

$[Ru(CO)(NO)(CH_3CN)(P^tBu_2Me)_2][BAr^F_4]$. A CH_2Cl_2 solution of $[Ru(CO)(NO)(P^tBu_2Me)_2][BAr^F_4]$ (50 mg, 0.037 mmol) and CH_3CN (2 μL, 0.038 mmol) was stirred for 5 min. The solvent was evaporated *in vacuo*, and the residue was dissolved in CH_2Cl_2. The solution was layered with pentane. After 12 h at −20 °C, orange crystals were obtained. Yield: 47 mg (92%). ^1H NMR ($CDCl_3$, 20 °C). δ 1.15 (two overlapping vt, J_{HP} = 7.4 Hz, 36H, P^{t}Bu). 1.49 (vt, J_{HP} = 3.3 Hz, 6H, PMe). 2.48 (s, 3H, CH_3CN), 7.50 (s, 4H, *p*-aryl), 7.70 (s, 8H, *o*-aryl). $^{31}P\{^1H\}$ NMR ($CDCl_3$, 20 °C): 47.4. IR ($CDCl_3$): ν_{CN} = 2257 cm^{-1}, ν_{CO} = 1960 cm^{-1}, ν_{NO} = 1609 cm^{-1}. Anal. Calcd for $RuC_{53}H_{57}BF_{24}N_2O_3P_2$: C, 45.47; H, 4.10; N, 2.00. Found: C, 45.62; H, 4.04; N, 2.10.

$[Ru(CO)(NO)(P^tBu_2Me)_2][B(C_6H_3\text{-}3,5\text{-}(CF_3)_2)_4]$ + H_2O. In an NMR tube fitted with a rubber septum, $[Ru(CO)(NO)(P^tBu_2Me)_2][BAr^F_4]$ (**3**, 10 mg, 7.4 × 10^{-3} mmol) was dissolved in $CDCl_3$ (0.5 mL). To this was added H_2O (0.4 μL, 2.2 mmol) via syringe. No significant color change was observed after the mixing. ^1H NMR ($CDCl_3$, 20 °C): δ 1.20 (vt, J_{HP} = 7.5 Hz, 18H, P^{t}Bu), 1.25 (vt, J_{HP} = 7.4 Hz, 18H, P^{t}Bu), 1.53 (vt, J_{HP} = 3.2 Hz, 6H, PMe), 2.20 (s, broad, H_2O), 7.50 (s, 4H, *p*-aryl), 7.70 (s, 8H, *o*-aryl). $^{31}P\{^1H\}$ NMR: 54.2 ppm. IR ($CDCl_3$) ν_{CO} = 1966 cm^{-1} (for **3**, $[Ru(CO)(NO)(P^tBu_2Me)_2][BAr^F_4]$), ν_{CO} = 1950 cm^{-1} (for $[Ru(CO)(NO)(OH_2)(P^tBu_2Me)_2][BAr^F_4]$), ν_{NO} = 1711 cm^{-1} (for **3**), ν_{NO} = 1607 cm^{-1} (for $[Ru(CO)(NO)(OH_2)(P^tBu_2Me)_2][BAr^F_4]$). Upon evaporation of the volatiles, $[Ru(CO)(NO)(P^tBu_2Me)_2][BAr^F_4]$ is recovered.

$RuF(CO)(NO)(P^tBu_2Me)_2$. A mixture of $RuCl(CO)(NO)(P^tBu_2Me)_2$ (100 mg, 0.19 mmol) and CsF (100 mg, 0.66 mmol) in acetone

(8) (a) Richter-Addo, G. B.; Legzdins, P. *Metal Nitrosyls*; Oxford University Press: New York, 1992. (b) Johnson, B. F. G.; Haymore, B. L.; Dilworth, J. R. In *Comprehensive Coordination Chemistry*; Wilkinson, G., Ed., 1987, Vol. 2, p 99.

(9) Brookhart, M.; Grant, B.; Volpe, A. F., Jr. *Organometallics* **1992**, *11*, 3920.

(10) Gill, D. F.; Shaw, B. L. *Inorg. Chim. Acta* **1979**, *32*, 19.

(5 mL) was stirred at room temperature for 18 h. After the evaporation of volatiles, the residue was extracted with pentane and filtered. The filtrate was concentrated to *ca.* 5 mL and cooled to −40 °C to afford orange crystals. Yield: 58 mg (61%). ^{1}H NMR ($CDCl_3$, 20 °C): δ 1.19 (vt, J_{HP} = 6.8 Hz, 18H, P^{t}Bu), 1.25 (vt, J_{HP} = 6.8 Hz, 18H, P^{t}Bu), 1.53 (vt, J_{HP} = 3.3 Hz, 6H, PMe). ^{31}P{^{1}H} NMR ($CDCl_3$, 20 °C): δ 52.2 (s) ppm. ^{19}F NMR ($CDCl_3$, 20 °C): −268.7 ppm (broad). IR ($CDCl_3$): ν_{CO} = 1912 cm^{-1}, ν_{NO} = 1568 cm^{-1}. Anal. Calcd for $C_{19}H_{42}FNO_2P_2Ru$: C, 45.77; H, 8.49; N, 2.81. Found: C, 46.47; H, 8.42; N, 3.22.

RuH(CO)(NO)(P^{t}Bu$_2$Me)$_2$. RuCl(CO)(NO)(P^{t}Bu$_2$Me)$_2$ (100 mg, 0.19 mmol) and $NaBH_4$ (20 mg, 0.53 mmol) were mixed with benzene (5 mL). To the mixture was slowly added methanol (0.5 mL), gas was evolved immediately upon the addition. The mixture changed color from red to pale orange. After the mixture was stirred for 1 h, the volatiles were removed *in vacuo* and the residue was extracted with pentane (10 mL) and filtered through a Celite pad. The filtrate was concentrated to *ca.* 1 mL and cooled in a −40 °C freezer for 12 h. Dark orange crystals formed and were filtered. Yield: 81 mg (89%). ^{1}H NMR (C_6D_6, 20 °C): δ 1.26 (vt, J = 6 Hz, 6H, PCH_3), 1.21 (two overlapping vt, J = 13.2 Hz, 36H, P^{t}Bu), −6.0 (t, J_{PH} = 22 Hz, 1H, RuH). ^{31}P{^{1}H} NMR (C_6D_6, 20 °C): δ 74.9 (s). IR (C_6D_6, cm^{-1}): ν(CO) = 1896 cm^{-1}, ν(NO) = 1616 cm^{-1}. Anal. Calcd for $C_{19}H_{43}NO_2P_2Ru$: C, 47.48; H, 9.02; N, 2.91. Found: C, 48.39; H, 9.18; N, 2.76.

X-ray Structure Determination. (a) Ru(FBF$_3$)(CO)(NO)(P^{t}Bu$_2$Me)$_2$. A crystal of suitable size was cleaved from a cluster of crystals. The crystal was mounted on a glass fiber with use of silicone grease and was then transferred to a goniostat where it was cooled to −168 °C for characterization and data collection. An automated search for peaks followed by analysis with the programs DIRAX and TRACER revealed a primitive orthorhombic cell. Following intensity data collection ($6° < 2\theta < 50°$), the additional conditions $l = 2n$ for $0k1$, $h = 2n$ for $h01$, and $k = 2n$ for $hk0$, uniquely determined space group *Pcab*. Four standard measured every 300 data showed no significant trends. The data were corrected for absorption (maximum and minimum factors: 0.841 and 0.910). The structure was solved by using a combination of direct methods (MULTAN78) and Fourier techniques. The position of the ruthenium atom was obtained from an initial E-map. The positions of the remaining atoms, including all of the hydrogens, were obtained from iterations of a least-squares refinement, followed by a difference Fourier calculation. In the final cycles of refinement, the non-hydrogen atoms were varied with anisotropic thermal parameters and the hydrogen atoms were varied with isotropic thermal parameters. In the final difference map, the largest peak was 0.62 and the deepest hole was −0.35 e/Å^3.

(b) [Ru(CO)(NO)(P^{t}Bu$_2$Me)$_2$][B(C$_6$H$_3$-3,5-(CF$_3$)$_2$)$_4$]. The sample consisted of elongated crystals which resembled hexagonal prisms. A small, nearly equidimensional fragment was cleaved from a well-formed crystal and affixed to the end of a glass fiber with use of silicone grease. The sample was then transferred to the goniostat where it was cooled to −165 °C for characterization and data collection ($6° < 2\theta < 45°$). Standard inert atmosphere handling techniques were used. A systematic search of a limited hemisphere of reciprocal space located a set of diffraction maxima with systematic monoclinic space group $P2_1/a$. The data were collected ($6° < 2\theta < 45°$) by using a standard moving crystal−moving detector technique with fixed backgrounds at each extreme of the scan. Data were corrected for Lorentz and polarization effects, and equivalent reflections were averaged. The structure was readily solved by direct methods (MULTAN78) and Fourier techniques. All non-hydrogen atoms were refined anisotropically in the full-matrix least-squares procedure. A difference Fourier map located the position of most hydrogen atoms, and all hydrogens were introduced as fixed atom contributors in the final cycles of refinement. When an occupancy factor is introduced and allowed to vary, the site numbered 22 converges to 23% carbon and that numbered 24 converges to 29% nitrogen. There is thus a nonrandom carbon/nitrogen disorder, although two positions could not be resolved for the disordered atoms at any one site. A final difference Fourier was featureless, the largest peaks, located at the F sites, being 0.8 e/Å^3.

(c) RuH(NO)(CO)(P^{t}Bu$_2$Me)$_2$. Crystal handling and data collection was analogous to the above two samples. Systematic absences uniquely determined space group $P2_1/n$. A small but significant variation in the intensities, as determined by four standards measured every 300 data, was corrected by using a locally written anisotropic drift correction program (DRIFT). No correction was made for absorption. The structure was solved by using a combination of direct methods (MULTAN78) and Fourier techniques. The positions of the Ru and P atoms were obtained from an initial E-map. The positions of the remaining non-hydrogen atoms were obtained from iterations of a least-squares refinement followed by a difference Fourier calculation. Hydrogens bonded to carbons were included in fixed calculated positions with thermal parameters fixed at one plus the isotropic thermal parameter of the parent carbon atom. An anticipated hydrogen bonded to Ru was not observed and was not included in the refinements. In the final cycles of refinement, the non-hydrogen atoms were varied with anisotropic thermal parameters, giving 227 total variables. The largest peak in the final difference map was 1.35, and the deepest hole was −0.85 e/Å^3.

Computational Details. *Ab initio* calculations were carried out on $RuX(CO)(NO)(PH_3)_2^+$ (X = Cl^-, BF_4^-, H^-, no ligand, NCH, CO) at the Becke3LYP computational level[11] with Gaussian 94.[12] Effective core potentials were used on the Ru,[13] P, and Cl atoms.[14] The basis set was of valence double-ζ quality,[13−15] supplemented with a shell of polarization d functions added on the P, Cl,[16] C, N, and O atoms.[17] Full geometry optimizations were carried out without symmetry constraint unless otherwise stated.

The two different isomeric forms corresponding to the two coordination modes of the nitrosyl ligand, bent or linear, were checked for each substituent X. This was accomplished through the choice of the starting geometry of the optimization process. This employed the X-ray structure of $Ru(FBF_3)(NO)(CO)(PH_3)_2$ for bent nitrosyl and a regular trigonal bipyramid (TBP) structure with two axial phosphines for linear nitrosyl. In some cases, both calculations converged to the same structure, while in other cases, two different isomeric forms were found.

Results

Preparation and Characterization of the Ruthenium Nitrosyl Complexes. Refluxing of an ethanol solution of RuHCl(CO)(P^{t}Bu$_2$Me)$_2$ and *N*-methyl-*N*-nitroso-*p*-toluenesulfonamide gives clean conversion to RuCl(CO)(NO)(P^{t}Bu$_2$Me)$_2$, **1**.[18] In an IR spectrum of **1**, a nitrosyl stretch is observed at fairly low frequency, suggesting coordination of a NO ligand in a bent fashion. Since the formal charge of a bent nitrosyl ligand can be treated as negative (NO^-), the formal oxidation state of the ruthenium in **1** should be regarded as +2.[19] In an isoelectronic iridium complex, $[IrCl(CO)(NO)(PPh_3)_2]^+$, a bent NO ligand was reported and the structure of the complex was described as square-pyramidal with a bent NO at an apical site.[20] A similar square-pyramidal structure is expected for complex

(11) (a) Becke, A. D. *J. Chem. Phys.* **1993**, *98*, 5648. (b) Lee, C.; Yang, W.; Parr, R. G. *Phys. Rev. B* **1988**, *37*, 785.

(12) Frisch, M. J.; Trucks, G. W.; Schlegel, H. B.; Gill, P. M. W.; Johnson, B. G.; Robb, M. A.; Cheeseman, J. R.; Keith, T.; Petersson, G. A.; Montgomery, J. A.; Raghavachari, K.; Al-Laham, M. A.; Zakrzewski, V. G.; Ortiz, J. V.; Foresman, J. B.; Peng, C. Y.; Ayala, P. Y.; Chen, W.; Wong, M. W.; Andres, J. L.; Replogle, E. S.; Gomperts, R.; Martin, R. L.; Fox, D. J.; Binkley, J. S.; Defrees, D. J.; Baker, J.; Stewart, J. P.; Head-Gordon, M.; Gonzalez, C.; Pople, J. A. *Gaussian 94*; Gaussian, Inc.: Pittsburgh, PA, 1995.

(13) Hay, P. J.; Wadt, W. R. *J. Chem. Phys.* **1985**, *82*, 299.

(14) Wadt, W. R.; Hay, P. J. *J. Chem. Phys.* **1985**, *82*, 284.

(15) Hehre, W. J.; Ditchfield, R.; Pople, J. A. *J. Chem. Phys.* **1972**, *56*, 2257−2261.

(16) Francl, M. M.; Pietro, W. J.; Hehre, W. J.; Binkley, J. S.; Gordon, M. S.; DeFrees, D. J.; Pople, J. A. *J. Chem. Phys.* **1982**, *77*, 3654.

(17) Hariharan, P. C.; Pople, J. A. *Theor. Chim. Acta* **1973**, *28*, 213.

(18) (a) Piper, T. S.; Wilkinson, G. *J. Inorg. Nucl. Chem.* **1956**, *3*, 104. (b) Laing, K. R.; Roper, W. R. *J. Chem. Soc. (A)* **1970**, 2149. (c) Johnson, B. F. G.; Segal, J. A. *J. Chem. Soc., Dalton Trans.* **1973**, 478.

(19) An analogous complex with **1**, RuCl(CO)(NO)(PPh$_3$)$_2$, was reported and described as a Ru(0) complex.[18b] However, the reported ν_{NO} value of the complex suggests that the NO ligand in the complex is also a bent NO with Ru(II), as in **1**.

(20) Hodgson, D. J.; Ibers, J. A. *Inorg. Chem.* **1968**, *7*, 2345.

Table 1. Crystallographic Data for $Ru(CO)(NO)(BF_4)(P^tBu_2Me)_2$

formula	$C_{19}H_{42}BF_4NO_2P_2Ru$	fw	566.37 g·mol^{-1}
a	16.178(4) Å	space group	*Pcab*
b	24.649(6) Å	*T*	−168 °C
c	13.141(3) Å	*λ*	0.71069 Å[a]
V	5240.14 Å^3	ρ_{calc}	1.436 g·cm^{-3}
Z	8	*μ*	7.64 cm^{-1}
$R(F_o)$[b]	0.0327	$R_w(F_o)$[c]	0.0328

[a] Graphite monochromator. [b] $R = \sum||F_o| - |F_c||/\sum|F_o|$. [c] $R_w = [\sum w(|F_o| - |F_c|)^2/\sum w|F_o|^2]^{1/2}$ where $w = 1/\sigma^2(|F_o|)$.

Table 2. Selected Bond Distances (Å) and Angles (deg) for $Ru(CO)(NO)(BF_4)(P^tBu_2Me)_2$

Distances			
Ru(1)−P(11)	2.4489(8)	F(2)−B(3)	1.451(4)
Ru(1)−P(21)	2.4559(7)	F(4)−B(3)	1.371(3)
Ru(1)−F(2)	2.2984(18)	F(5)−B(3)	1.3685(9)
Ru(1)−N(9)	1.8395(21)	F(6)−B(3)	1.375(4)
Ru(1)−C(7)	1.8020(25)	O(8)−C(7)	1.161(3)
		O(10)−N(9)	1.190(3)

Angles			
P(11)−Ru(1)−P(21)	167.849(25)	N(9)−Ru(1)−C(7)	103.11(12)
P(11)−Ru(1)−F(2)	85.12(5)	Ru(1)−F(2)−B(3)	160.75(10)
P(11)−Ru(1)−N(9)	94.63(7)	Ru(1)−N(9)−O(10)	135.61(15)
P(11)−Ru(1)−C(7)	92.01(9)	Ru(1)−C(7)−O(8)	178.0(3)
P(21)−Ru(1)−F(2)	87.57(4)	F(2)−B(3)−F(4)	105.66(27)
P(21)−Ru(1)−N(9)	96.03(7)	F(2)−B(3)−F(5)	108.99(24)
P(21)−Ru(1)−C(7)	91.24(7)	F(2)−B(3)−F(6)	108.63(14)
F(2)−Ru(1)−N(9)	98.37(8)	F(4)−B(3)−F(5)	110.74(14)
F(2)−Ru(1)−C(7)	158.49(10)	F(4)−B(3)−F(6)	111.66(24)
		F(5)−B(3)−F(6)	110.97(28)

1 with Ru(II). The color of the complex is reddish orange, which is consistent with the coordinatively unsaturated character of the complex. Only one signal is observed in a $^{31}P\{^1H\}$ NMR spectrum, and the ^{t}Bu groups of the phosphines are detected as two virtually-coupled triplets in a ^{1}H NMR spectrum, consistent with no mirror plane of symmetry perpendicular to the RuCl(CO)(NO) plane.

Addition of equimolar $AgBF_4$ to a solution of **1** in benzene, toluene, CH_2Cl_2, or THF causes immediate precipitation of AgCl to give $Ru(FBF_3)(CO)(NO)(P^tBu_2Me)_2$, **2**, quantitatively. This complex is quite thermally stable, at least up to 100 °C, and recrystallizable from hot toluene. Complex **2** is moderately soluble in benzene and toluene, and it is slightly soluble even in nonpolar alkanes (pentane and hexane). The solubility of **2** indicates coordination of a BF_4^- anion to the ruthenium in **2**. An IR spectrum of **2** in CD_2Cl_2 gives an NO stretching vibration at 1572 cm^{-1}. This value is low, and consistent with a bent nitrosyl as observed in complex **1**. The BF_4^- ligand is coordinating very weakly and shows rapid exchange of dangling and coordinated F. In its ^{19}F NMR spectra, only one signal is observed at δ −161 between 20 and −90 °C. The resonance is very sharp at 20 °C ($w_{1/2}$ = 8.5 Hz), and even at −90 °C it does not decoalesce into two signals, which are expected for a coordinating BF_4^- with a slow exchange process.[21] However, at −90 °C, the signal is very broad ($w_{1/2}$ = 321 Hz). The X-ray single-crystal structure determination (Tables 1 and 2) of **2** confirms η^1-BF_4^- coordination and bent NO in the solid state.

As its solubility indicated, complex **2** is a molecular species with a square-pyramidal geometry (Figure 1). A bent (135.6°) nitrosyl ligand occupies the apical position and a very weakly bonded BF_4^- (Ru−F = 2.298(2) Å) is *trans* to CO in an η^1-bonding mode. Thus, this molecule prefers a 16-electron configuration to an 18-electron one, either via η^2-BF_4^- or by a linear NO ligand. The Ru−F bond is long, but still this perturbs

(21) Beck, W.; Sünkel, K. *Chem. Rev.* **1988**, *88*, 1405 and references therein.

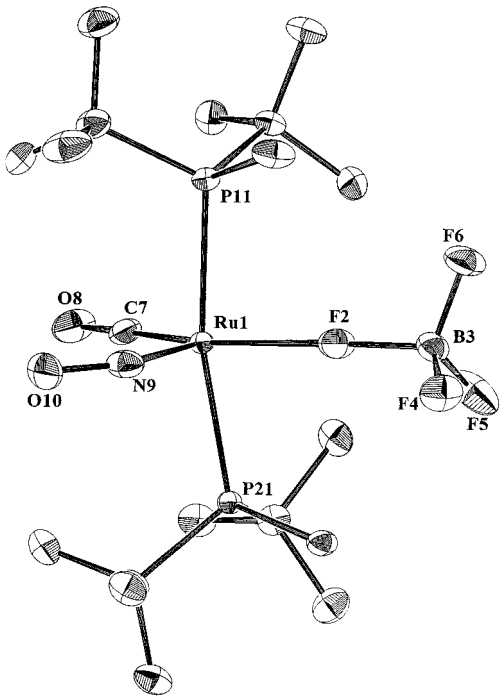

Figure 1. ORTEP drawing of the non-hydrogen atoms of $Ru(FBF_3)(CO)(NO)(P^tBu_2Me)_2$, showing selected atom labeling.

the BF bond lengths to make B−μ−F longer (1.451(4) Å) than the other three B−F bonds (1.372(5) Å). The Ru−F−B angle is very large (160.75(10) Å).

The Cl^- ligand in **1** and the BF_4^- in **2** are very labile and easily replaced with noncoordinating anion $B[C_6H_3\text{-}3,5\text{-}(CF_3)_2]_4^-$ ($BAr^F{}_4^-$) by an $NaBAr^F{}_4$ treatment in dichloromethane, to give a four-coordinate cationic complex $[Ru(CO)(NO)(P^tBu_2Me)_2][BAr^F{}_4]$, **3**. The PPh_3 analog $Ru(CO)(NO)(PPh_3)_2^+$ was previously proposed as an undetected intermediate.[18c] The choice of CH_2Cl_2 as a solvent for this anion exchange is important, since the reaction does not proceed in benzene, toluene, or THF. A similar solvent dependency was observed for an analogous anion exchange reaction between $RuH(OSO_2CF_3)(CO)(P^tBu_2Me)_2$ and $NaBAr^F{}_4$.[22] The nitrosyl ligand in complex **3** gives its IR absorption at 1709 cm^{-1}; this value is much higher than those in **1** and **2** and within the range for those of linear nitrosyl groups. Thus, complex **3** is another example of an extremely rare coordinatively-unsaturated Ru(0) species.[1] Complex **3** shows two virtual triplets for the ^{t}Bu groups of the phosphine in the ^{1}H NMR spectrum and one singlet in the $^{31}P\{^1H\}$ NMR spectrum at room temperature. All these spectroscopic observations are consistent with a nonplanar structure of **3**, which is analogous to that of $Ru(CO)_2(P^tBu_2Me)_2$.[1] In particular, two ^{t}Bu chemical shifts *excludes* a planar geometry at Ru.

In marked contrast to **2**, complex **3** is an ionic species; the crystals of **3** (Tables 3 and 4) contain $[Ru(CO)(NO)(P^tBu_2Me)_2]^+$ cation (Figure 2) and $BAr^F{}_4^-$ anion with a solvent molecule (CH_2Cl_2) per formula unit. The fact that this solvent is *not* bound to the metal shows that unsaturated Ru in this cation is not a strong σ Lewis acid. The cation has a nonplanar coordination geometry with a P−Ru−P angle of 157.33(8)°; in $Ru(CO)_2(P^tBu_2Me)_2$, this angle is 165.56(8)°. The N−Ru−C angle (120.4(3)°) is smaller than the C−Ru−C angle in $Ru(CO)_2(P^tBu_2Me)_2$ (133.3(4)°). While there is potential for disorder between NO and CO, the lattice CH_2Cl_2 molecule points one of its hydrogens toward O(25) in a weak hydrogen

(22) Huang, D.; Caulton, K. G. Unpublished results.

Table 3. Crystallographic Data for $[Ru(CO)(NO)L_2][BAr^F_4]$

formula	$C_{52}H_{56}RuO_2NBF_{24}P_2Cl_2$	fw	1427.72 g·mol^{-1}
a	18.897(2) Å	space group	$P2_1/a$
b	16.897(2) Å	*T*	−170 °C
c	19.355(2) Å	*λ*	0.71069 Å[a]
β	97.79(1)	ρ_{calc}	1.549 g·cm^{-3}
V	6123.02 Å^3	*μ*	4.99 cm^{-1}
Z	4	$R(F_o)$[b]	0.0566
	$R_w(F_o)$[c]	0.0507	

[a] Graphite monochromator. [b] $R = \sum||F_o| - |F_c||/\sum|F_o|$. [c] $R_w = [\sum w(|F_o| - |F_c|)^2/\sum w|F_o|^2]^{1/2}$ where $w = 1/\sigma^2(|F_o|)$.

Table 4. Selected Bond Distances (Å) and Angles (deg) for $Ru(CO)(NO)(P^tBu_2Me)_2^+$

Distances			
Ru(1)−P(2)	2.39966(28)	Ru(1)−C(24)	1.8141(15)
Ru(1)−P(3)	2.3949(28)	O(23)−N(22)	1.164(10)
Ru(1)−N(22)	1.806(9)	O(25)−C(24)	1.152(4)

Angles			
P(2)−Ru(1)−P(3)	157.33(8)	Ru(1)−P(2)−C(5)	119.4(3)
P(2)−Ru(1)−N(22)	94.4(3)	Ru(1)−P(2)−C(9)	104.8(3)
P(2)−Ru(1)−C(24)	95.7(3)	Ru(1)−P(3)−C(13)	107.2(3)
P(3)−Ru(1)−N(22)	95.9(3)	Ru(1)−P(3)−C(14)	119.4(3)
P(3)−Ru(1)−C(24)	96.3(3)	Ru(1)−P(3)−C(18)	106.2(3)
N(22)−Ru(1)−C(24)	120.4(3)	Ru(1)−N(22)−O(23)	161.63(22)
Ru(1)−P(2)−C(4)	107.5(3)	Ru(1)−C(24)−O(25)	159.9(8)

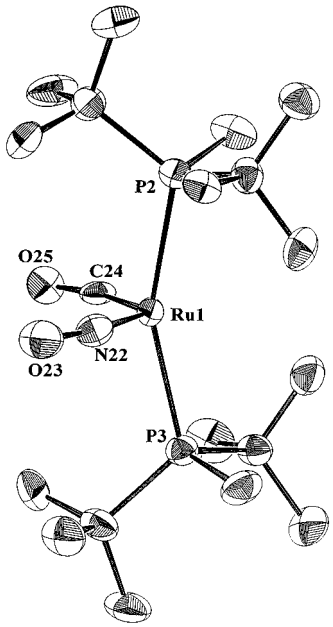

Figure 2. ORTEP drawing of the non-hydrogen atoms of $Ru(CO)(NO)(P^tBu_2Me)_2^+$. Unlabeled atoms are carbons.

bond. This may be the reason why the refinement of X-ray data is consistent with ∼80% occupancy of N at the "nitrogen" site attached to O(23); similarly, there is only ∼80% occupancy of carbon at the C(24) site, the remainder being nitrogen. That is, CH_2Cl_2 distinguishes the sites which are otherwise equivalent in the isolated cation, and inhibits random disorder. While the X-ray refinement argues for an ordered structure, the Ru−C/N bond lengths (short at 1.81 Å) and Ru−C/N−O bond angles (160°) are so similar for the two sites that we take the conservative approach and decline to draw chemical conclusions from these parameters. The Ru−P−C angle to each ^{t}Bu group which is *syn* to the Ru(CO)(NO) hemisphere is over 12° larger than the other four Ru−P−C angles. The analogous effect is seen in $Ru(CO)_2(P^tBu_2Me)_2$.[1] However, each PR_3 group is staggered with respect to the Ru(CO)(NO)P 3-fold rotor. The structure of the anion is unexceptional.

Table 5. Crystallographic Data for $[RuH(CO)(NO)L_2]$

formula	$C_{19}H_{42}NO_2P_2Ru$	fw	480.7 g·mol^{-1}
a	12.761(2) Å	space group	$P2_1/n$
b	14.022(2) Å	*T*	−168 °C
c	14.944(2) Å	*λ*	0.71069 Å[a]
β	114.40(1)°	ρ_{calc}	1.31 g·cm^{-3}
V	2435.20 Å^3	*μ*	7.87 cm^{-1}
Z	4	$R(F_o)$[b]	0.0423
	$R_w(F_o)$[c]	0.0407	

[a] Graphite monochromator. [b] $R = \sum||F_o| - |F_c||/\sum|F_o|$. [c] $R_w = [\sum w(|F_o| - |F_c|)^2/\sum w|F_o|^2]^{1/2}$ where $w = 1/\sigma^2(|F_o|)$.

Table 6. Selected Bond Distances (Å) and Angles (deg) for $RuH(NO)(CO)(P^tBu_2Me)_2$

Distances			
Ru(1)−P(6)	2.3617(13)	Ru(1)−C(4)	1.8883(17)
Ru(1)−P(16)	2.3605(12)	O(3)−N(2)	1.1995(20)
Ru(1)−N(2)	1.8010(18)	O(5)−C(4)	1.1583(22)

Angles			
P(6)−Ru(1)−P(16)	159.17(4)	Ru(1)−P(6)−C(11)	113.89(17)
P(6)−Ru(1)−N(2)	98.81(14)	Ru(1)−P(6)−C(15)	111.68(15)
P(6)−Ru(1)−C(4)	89.97(17)	Ru(1)−P(16)−C(17)	113.95(15)
P(16)−Ru(1)−N(2)	96.37(13)	Ru(1)−P(16)−C(21)	113.75(12)
P(16)−Ru(1)−C(4)	88.76(14)	Ru(1)−P(16)−C(25)	111.69(16)
N(2)−Ru(1)−C(4)	136.52(19)	Ru(1)−N(2)−O(3)	174.2(3)
Ru(1)−P(6)−C(7)	114.26(14)	Ru(1)−C(4)−O(5)	178.2(4)

Although complex **3** does not interact with CH_2Cl_2, it coordinates H_2O, CH_3CN, CO, F^-, and H^-. In the presence of excess H_2O, a fast equilibrium is established between $[Ru(CO)(NO)L_2]^+$ and $[Ru(CO)(NO)(OH_2)L_2]^+$; at 20 °C, only one singlet is seen in the $^{31}P\{^1H\}$ NMR spectrum of the mixture. However, the solution IR spectrum distinctly reveals the presence of **3** and its H_2O adduct. The latter has lower ν_{CO} (1950 cm^{-1}) and ν_{NO} (1607 cm^{-1}; i.e., 100 cm^{-1} lower). The H_2O is only weakly coordinated since upon removal of the reaction solvent *in vacuo*, only **3** is recovered in the residue. The stronger donor ligand CH_3CN does coordinate with **3** irreversibly to give $[Ru(CO)(NO)(CH_3CN)L_2][BAr^F_4]$, which also shows a lower NO stretching frequency than **3**. However, the CO stretching is only slightly lower than that of **3**, indicating that the NO stretching is more sensitive to the electron density of Ru. The strong π acid CO coordinates to **3** to give $[Ru(CO)_2(NO)L_2][BAr^F_4]$, which shows much higher ν_{CO} (2047, 1996 cm^{-1}) and ν_{NO} (1738 cm^{-1}) values. The high NO stretching frequency supports the presence of a linear Ru−N−O.

Anionic nucleophiles F^- (CsF) and H^- (NaH) also react with **3** to form $RuF(CO)(NO)L_2$ and $RuH(CO)(NO)L_2$, respectively. They can be more economically and conveniently prepared from $RuCl(CO)(NO)L_2$ by salt metathesis with CsF or by reaction with $NaBH_4$. $RuF(CO)(NO)L_2$ shows a broad ^{19}F NMR singlet at 268.7 ppm. The ν_{NO} value is low (1568 cm^{-1}), consistent with a bent RuNO. The hydride chemical shift value (−6 ppm) of $RuH(CO)(NO)L_2$ indicates that the hydride is not *trans* to a vacant site. The most noteworthy feature of this complex is that it has the lowest ν_{CO} (1896 cm^{-1}) among the complexes $RuX(CO)(NO)L_2$, indicating an electron-rich metal center. However, the ν_{NO} (1616 cm^{-1}) is higher than that of $Ru(FBF_3)(CO)(NO)L_2$. To determine the geometry of this complex and to shed light on this apparent paradox, a single-crystal X-ray structure determination was carried out.

The X-ray structure determination of $RuH(NO)(CO)L_2$ (Tables 5 and 6), while it did not locate the hydride ligand, is wholly consistent with a trigonal bipyramidal (TBP) structure with linear (Ru−N−O = 174.2(3)°) nitrosyl and two axial phosphines (Figure 3). The Ru−N distance is significantly (49 σ) shorter than the Ru−C distance, consistent with NO^+ as a very strong

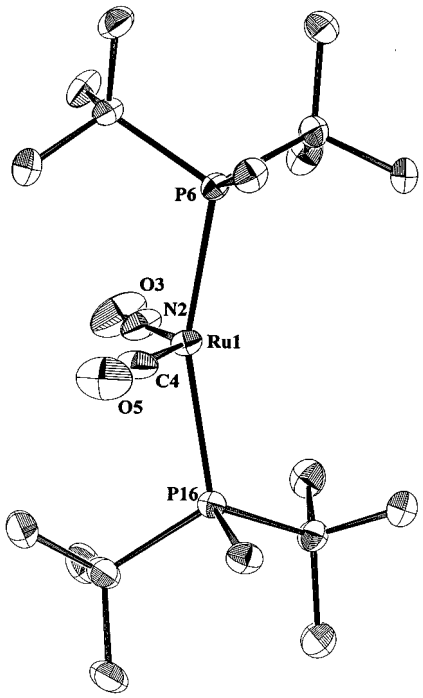

Figure 3. ORTEP drawing of the non-hydrogen atoms of RuH(NO)(CO)(P^tBu_2Me)$_2$. The hydride was not located. Unlabeled atoms are carbons.

π-acid. The C−Ru−N angle (136.52(19)°) is consistent with an equatorial/equatorial angle in a TBP (and is too small for a basal/basal angle in a square pyramid). The phosphine ligands (P−Ru−P = 159.17(4)°) bend toward the (equatorial) site where the small hydride is proposed to reside, and all P−Ru−N or C angles are within 5° of their average value, 94°. The substituents on the phosphines are staggered with respect to the RuH(NO)(CO) unit. The methyl substituents are then directly opposed to each other.

It is of interest to compare the structural parameters of RuH(NO)(CO)L_2 to those of its (formal) H^- removal product, Ru(NO)(CO)L_2^+. Since the hydride of RuH(NO)(CO)L_2 is not located in the X-ray structural study, the ORTEP diagram of RuH(NO)(CO)L_2 (Figure 3) is very similar to that of Ru(NO)(CO)L_2^+ (Figure 2). Both of them adopt TBP geometry with one equatorial ligand either very small or missing. The P−Ru distances are close (2.36 *vs* 2.39 Å). The same is true for the P−Ru−P angles (159.17(4)° *vs* 157.33(8)°), which are bent away from the Ru(NO)(CO) hemisphere. However, the differences between these structures are significant. The Ru−N−O and Ru−C−O angles are bent in Ru(NO)(CO)L_2^+, while they are linear (174°) in RuH(NO)(CO)L_2. Moreover, one ^{t}Bu group of each phosphine ligand is bent toward the vacant site in Ru(NO)(CO)L_2^+. In contrast, the ^{t}Bu groups of RuH(NO)CO)L_2 are pointing away from the missing hydride site. The Ru−P−C angles in RuH(NO)(CO)L_2 are the same (114°), in agreement with a hydride occupying the third equatorial site; this contrasts to molecules where a ^{t}Bu group on L agostically binds to an unsaturated metal. From Ru(NO)(CO)L_2^+ to RuH(NO)(CO)L_2, the oxidation states of Ru remain the same (zero), while the Ru electron count increases by two (from 16e to 18e). This change is also reflected in the bond length difference of NO and CO in the two molecules. RuH(NO)(CO)L_2 has a longer N−O (1.1995(20) Å) than that of Ru(NO)(CO)L_2^+ (average distance of N−O and C−O is 1.158 Å). The origin of this difference is the stronger π-donor ability of Ru in RuH(NO)(CO)L_2 than that in Ru(NO)(CO)L_2^+. This is consistent with the lower IR stretching frequencies of NO (1614 cm^{-1}) and CO (1896 cm^{-1}) in RuH(NO)(CO)L_2 than that in Ru(NO)(CO)L_2^+ (ν(NO) = 1709 cm^{-1}, ν(CO) = 1966 cm^{-1}).

Scheme 2

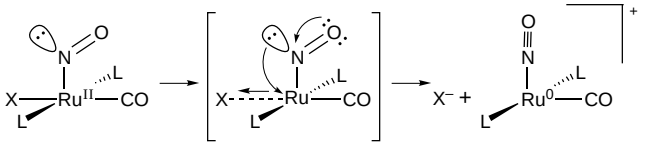

Solution Behavior of the Complexes. As mentioned in the previous section, the chloride ligand in **1** is very labile. Since the complex **1** is assigned as a 16-electron complex with the bent NO, the lability of the Cl^- ligand seems somewhat unusual, because, in general, a ligand dissociation gives a more electron-deficient species, i.e., a 14-electron species might be expected as a product of a Cl^- dissociation from a 16-electron complex. However, in this particular system, this is not the case. The product of the Cl^- dissociation from **1**, [Ru(CO)(NO)(P^tBu_2-Me)$_2$]$^+$, is a 16-electron species because, as a result of Cl^- dissociation, the nitrosyl ligand alters its coordination mode from bent (NO^-) to linear (NO^+), and the oxidation state of the ruthenium center changes from +2 to 0.[23] Thus, the Cl^- dissociation can be treated as an *intramolecular redox process*. The lability of the Cl^- ligand in **1** is thus assisted by a lone pair on the nitrogen atom of the bent NO, as illustrated in Scheme 2. Analogous correlations of electron counts of complexes and coordination modes of NO can be seen in the anion exchange (reaction with $NaBAr^F{}_4$) which converts **2** to **3**. Such a redox change, with NO bending, was reported earlier, and has been termed "stereochemical control of valence".[24]

The lability of the Cl^- in **1** is confirmed by $^{31}P\{^1H\}$ NMR spectroscopy. A mixture of **1** and **3** in CD_2Cl_2 gives only one *very sharp* resonance in its $^{31}P\{^1H\}$ NMR spectrum at room temperature. For a mixture of **1**:**3** = 0.6:0.4 molar ratio, a signal is detected at δ 50.1, and for **1**:**3** = 0.05:0.95 at δ 58.7. The signals of the mixtures are observed at weighted averages of the chemical shifts of pure **1** (δ 45.3) and **3** (δ 59.6), which indicate a rapid anion exchange between **1** and **3** at room temperature. In the IR spectrum (faster technique) of these solutions, the ν_{CO} and ν_{NO} vibrations assignable to both **1** and **3** are detected as clearly separated signals, which indicates coexistence of the two complexes independently in solution (no dimerization, no oligomerization, etc.). At −90 °C, the single $^{31}P\{^1H\}$ NMR signal decoalesced into several resonances and the spectrum shows a fairly complicated pattern. At this temperature, in addition to a slow chloride exchange between the two complexes, rotations around the Ru−P axis in both species are slow,[25] which gives two rotamers.

The solution behavior of the four-coordinate complex **3** was examined in toluene-d_8, diglyme-d_{14}, and $CDCl_2CDCl_2$ with variable-temperature ^1H NMR spectroscopy. The two ^{t}Bu groups of the phosphines of **3** are diastereotopic due to the nonplanarity of the complex. Indeed, complex **3** shows two virtual triplets for the ^{t}Bu groups on the phosphines in the ^1H NMR spectrum at room temperature in CD_2Cl_2, which is consistent with retention of its nonplanar structure even in solution. However, as the temperature is increased, the two signals become broader and then turn into a single broad resonance at and above 100 °C in toluene-d_8 (see Figure 4; the spectra are phosphorus decoupled for clarity). The broadening

(23) Chang, J.; Bergman, R. G. *J. Am. Chem. Soc.* **1987**, *109*, 4298.
(24) Enemark, J. H.; Feltham, R. D. *Proc. Natl. Acad. Sci. U.S.A.* **1972**, *69*, 3534. See also: Song, J.; Hall, M. B. *J. Am. Chem. Soc.* **1993**, *115*, 327.
(25) Notheis, J. U.; Heyn, R. H.; Caulton, K. G. *Inorg. Chim. Acta* **1995**, *229*, 187.

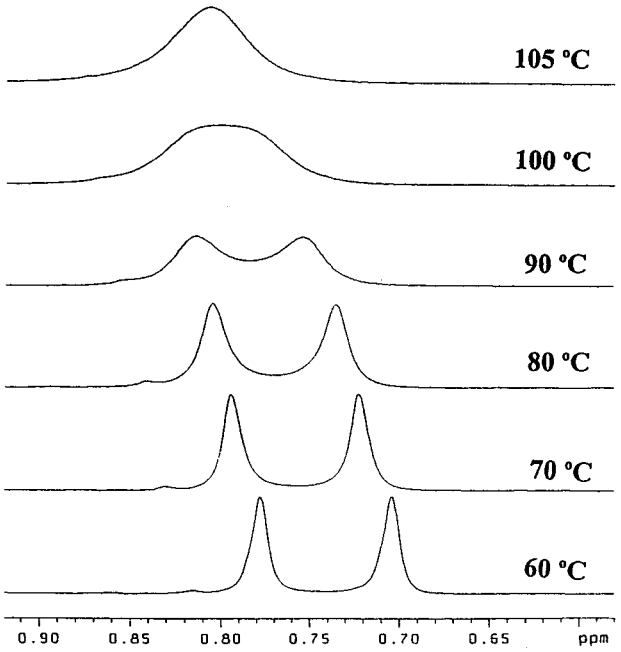

Figure 4. Variable-temperature $^1H\{^{31}P\}$ NMR spectra of **3** in toluene-d_8 at 400 MHz in the ^{t}Bu region.

and coalescence process is reversible in temperature and can be explained by fluxionality of complex **3** in solution. The inversion of the bent OC−Ru−NO unit as illustrated in Scheme 1, which makes the two ^{t}Bu groups magnetically equivalent, accounts for the VT ^1H NMR observations. The transition state of the fluxional process is a square-planar structure.

However, the solution behavior of **3** in toluene is not as simple as shown in Scheme 1. While the ^1H NMR spectrum of [Ru(CO)(NO)L_2]$BAr^F{}_4$ in $CDCl_3$ is consistent with one species being present, in C_6D_6 and toluene-d_8 at 25 °C, there are signals for two aryl groups and two PMe and four P^{t}Bu groups. These two species have comparable population, even in their two distinct (by 0.27 ppm, with baseline resolution) ^{19}F NMR signals; two $^{31}P\{^1H\}$ NMR signals are resolved by 0.05 ppm. We attribute these to distinct ion pairs in the low dielectric solvent. By 60 °C, the PMe and P^{t}Bu and aryl resonances have coalesced into half the number of signals, and from 60 to 90 °C, the ^{t}Bu signals change chemical shift significantly (∼0.05 ppm), consistent with altered populations of two rapidly equilibrating ion pair forms. From 90 to 105 °C, the two ^{t}Bu resonances coalesce to a single signal. Thus, the solution behavior of **3** should be explained as a combination of the OC−Ru−NO inversion and this ion pairing equilibrium.

The activation energy of the observed fluxional process in toluene is estimated as $\Delta G^{\ddagger}$ (at 100 °C) = 19.1 kcal mol^{-1}.[26] This value represents only an *upper limit* of the energy difference between the ground state (tetrahedral structure) and the transition state (planar structure), since some portion of the $\Delta G^{\ddagger}$ value should be attributed to the energy of breaking the ion pair interaction between the cation and the anion. In diglyme-d_{14}, the complex does not show any coalescence in its ^1H NMR up to 140 °C. Interaction of the solvent molecule (even coordination) with the Ru center in **3** (which is stronger than its interaction with $BAr^F{}_4^-$ in toluene) apparently prevents the inversion of the OC−Ru−NO moiety. Although a similar fluxional process is suspected from high-temperature ^1H NMR measurements of **3** in $CDCl_2CDCl_2$, detailed analyses of the behavior of **3** in $CDCl_2CDCl_2$ are uncertain because of slow decomposition of the complex at higher temperature in this solvent.

Reactivity of the Complexes. The BF_4^- ligand in **2** is extremely labile, and complex **2** shows reactivity analogous to that of the cation in **3**. It reacts with CO to give an ionic complex [Ru(CO)$_2$(NO)(P^{t}Bu$_2$Me)$_2$]BF_4, **4**, with a linear NO, not Ru(FBF$_3$)(CO)$_2$(NO)(P^{t}Bu$_2$Me)$_2$ with a bent NO; the reaction is very fast and quantitative, and in toluene or THF, complex **4** precipitates from a clear solution following introduction of CO. The ^{t}Bu groups of the phosphines appear as *one* virtually-coupled triplet in the ^1H NMR spectrum, consistent with the five-coordinate trigonal bipyramidal cationic form. The IR spectrum of **4** shows a strong ν_{NO} band at 1738 cm^{-1}, as expected for the linear NO ligand, in addition to two CO stretches with unequal intensities at 2047 and 1996 cm^{-1}. One of the two carbonyls of **4** is very labile, thus complex **4** is stable only under a CO atmosphere. Under Ar (or N_2), complex **4** releases a CO ligand to reform **2**. This observation shows that BF_4^- is competitive with CO in this system.

Complex **2** also reacts with equimolar acetonitrile. Addition of 1.1 equiv of MeCN to a CD_2Cl_2 solution of **2** converts the complex completely into a new species judging from ^1H, $^{31}P\{^1H\}$ NMR, and IR spectroscopy. The product shows its NO stretch at 1597 cm^{-1}, which is in a region for bent nitrosyls. The ^1H NMR signal for acetonitrile is observed as a broad singlet and is not resolved into those for coordinated and free MeCN. MeCN is interacting with the ruthenium weakly and rapidly exchanging with free MeCN. No precipitate is observed on adding acetonitrile. From these observations, we suggest a formula of the product as Ru(NCMe)(FBF$_3$)(CO)(NO)(P^{t}Bu$_2$Me)$_2$.

Unlike BF_4^- in **1**, the $BAr^F{}_4^-$ counteranion in **3** is not a potential ligand to the coordinatively unsaturated metal center. Thus, there is no competition between the added nucleophile (CO and MeCN) and the anion, and both CO and MeCN react with **3** irreversibly to form the corresponding products as isolable species.

The cationic complex **3** is more electrophilic, and a weaker reductant than Ru(CO)$_2$(P^{t}Bu$_2$Me)$_2$. Even though it is isoelectronic and isostructural with Ru(CO)$_2$(P^{t}Bu$_2$Me), its reaction pattern is completely different from the dicarbonyl analogue. It coordinates simple σ-donors such as MeCN or H_2O to give corresponding five-coordinate Ru(0) complexes. It does not oxidatively add H_2 or PhCCH. All these reaction patterns are completely different from those of Ru(CO)$_2$(P^{t}Bu$_2$Me)$_2$.

Computational Studies

Structure of RuX(CO)(NO)(PH$_3$)$_2$. Two structures are possible (Table 7), corresponding to either a 16-electron (d^6 Ru(II)) complex with bent NO and a square pyramidal (SP) Ru or to an 18-electron complex (d^8 Ru(0)) with linear NO and a trigonal bipyramidal (TBP) metal. A search for the two types of structures was carried out for each case (X).

For comparison, the molecule $CoCl_2(NO)(PR_3)_2$ appears to exist in solution as two isomers, one with linear and one with bent NO, but none of the molecules reported here have this feature.[27]

RuCl(CO)(NO)(PH$_3$)$_2$. Only one minimum (Figure 5) corresponding to an SP with an apical bent NO ligand (Ru−N−O 129.3°) was located.[28] The metal is significantly displaced

(26) The value was calculated from a chemical shift difference between the two ^{t}Bu signals and the coalesced temperature of the two signals, using the equation $k = \pi(\Delta\delta)(2)^{-1/2}$ and the Eyring equation.

(27) Brock, C. P.; Collman, J. P.; Dolcetti, G.; Farnham, P. H.; Ibers, J. A.; Lester, J. E.; Reed, C. A. *Inorg. Chem.* **1973**, *12*, 1304.

(28) Related results for Os have been obtained by M. P. Sigalas, personal communication.

Table 7. Selected Experimental and Theoretical Values for Some Angles of $RuX(CO)(NO)(PR_3)_2$ Systems[a]

	exp			SP		TBP		
X	ν_{NO}	N−Ru−C	Ru−N−O	N−Ru−C	Ru−N−O	N−Ru−C	Ru−N−O	E(TBP) − E(SP)
F^-	1568							*c*
Cl^-	1570			96.9	129.3			*c*
BF_4^-	1572	103.1	135.7	98.8	128.4			*c*
H_2O	1607							*c*
RCN	1609			97.8	125.8	116.1	154.2	+5.14
−	1709	120.4	161.5			120.0	147.6	
CO	1738			94.0[b]		121.8	130.3	180.0	+1.26
H^-	1616	136.5	174.2	97.1	129.3	133.7	171.6	−0.02

[a] Results are given for the two different computed minima, SP and TBP. Frequencies are in cm^{-1}, angles in degrees, and energies in kcal/mol. [b] Average value. [c] TBP is not a minimum.

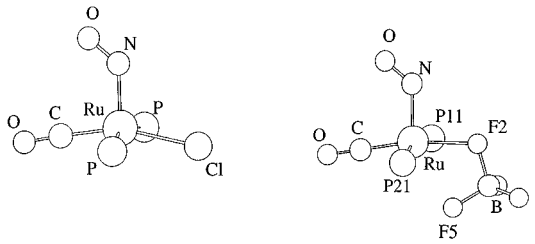

Figure 5. Becke 3LYP optimized structures of $RuCl(CO)(NO)(PH_3)_2$ and $Ru(BF_4)(CO)(NO)(PH_3)_2$.

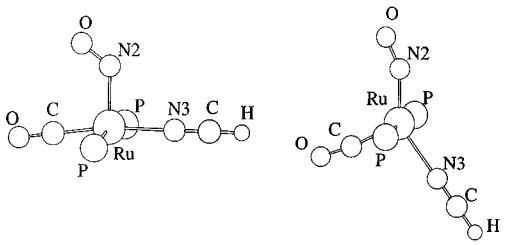

Figure 6. Becke 3LYP optimized structures of $Ru(NCH)(CO)(NO)(PH_3)^+$, showing SP (left) and TBP forms.

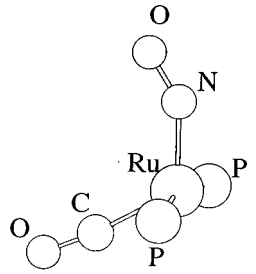

Figure 7. Becke 3LYP optimized structure of $Ru(CO)(NO)(PH_3)_2^+$.

from the plane of the equatorial ligand (Cl−Ru−C = 160.1°; P−Ru−P = 159.9°). There is C_s symmetry, with the mirror plane containing Cl, Ru, CO, and NO. The nitrosyl is bent toward CO. No TBP structure was located as a minimum on the potential energy surface (PES).

$Ru(BF_4)(CO)(NO)(PH_3)_2$. One minimum (Figure 5 and Table 7), corresponding to an SP with an apical bent NO (Ru−N−O = 128.4°), was located. The calculated structural parameters around the metal compare well to the experimental results. The most significant disagreement between calculated and experimental geometry concerns the way BF_4 is bound to the metal. While the large experimental Ru−F−B angle (160.7°) clearly suggests an η^1-coordinated BF_4^-, the much smaller calculated angle (103.2°) might be indicative of an η^2-BF_4. The calculated Ru−F2 distance is 2.234 Å, and the Ru−F5 distance is 2.598 Å. Despite this latter distance, we do not view BF_4 as a dihapto ligand. This point of view is supported by the following computational results. Atom F5 does not lie in the Ru(CO)(NO) plane, and the 20° dihedral angle between this plane and that of F2−B−F5 is too large to be viewed as a slight distortion away from the octahedral geometry expected for a d^6 hexacoordinated species. Moreover, forcing a coplanar arrangement between the two Ru−F bonds and the Ru−C and Ru−N bonds leads to an optimized structure only 1.4 kcal·mol^{-1} above the previous one. A much steeper energy rise would have been expected for a real bonding situation between Ru and F5. We thus view the BF_3 moiety as essentially freely rotating around the F2−B bond.

We explored further the bonding property of BF_4 ligand by searching for additional factors which could contribute to the large Ru−F−B angle. Steric factors come to mind as an obvious deficiency in the PH_3 model system. We thus calculated the entire species $Ru(BF_4)(CO)(NO)(P^tBu_2Me_2)$ at the IMOMM(Becke3LYP:MM3) level[29] and obtained no significant change in our optimized structure.

Despite the discrepancy around the BF_4 ligand, the structural results were good around the Ru center. To explore further the relationship between the coordination around Ru and the geometry of BF_4, the structure with an enforced 160.7° Ru−F2−B angle was optimized. This results in no significant change of geometry around Ru. This last result adds support to our interpretation of BF_4 as a monohapto ligand.

$[Ru(NCH)(CO)(NO)(PH_3)_2]^+$. Two isomeric structures (Figure 6) were located as minima on the PES. The most stable structure corresponds to an SP with an apical bent NO (Ru−N−O = 125.8°). As in the previous complexes, the angles between *trans* ligands are significantly less than 180° (N8−Ru−C = 171.9°; P−Ru−P = 166.5) and the symmetry is C_s. The NO ligand is bent toward CO. The other isomer, 5.1 kcal·mol^{-1} above the previous structure, is a TBP with axial phosphines. The angles within the equatorial plane are significantly distorted from ideal TBP (N(O)−Ru−C = 116.1°; N(O)−Ru−N(CH) = 143.3°). Interestingly, the NO ligand coordination is not really linear since Ru−N−O = 154.2°. We will return to these results in the discussion.

$[Ru(CO)(NO)(PH_3)_2]^+$. One minimum (Figure 7) is located for this tetracoordinated species. Due to structural disorder between NO and CO in our isolated solid, caution should be used when comparing these experimental with calculated geometrical parameters. The P−Ru−P and C−Ru−N angles, which are not affected by disorder, compare well to experiment (calculated [experimental] P−Ru−P, 166.6° [157.3°], N−Ru−C, 120.0° [120.4°]). According to the calculations, CO should be bound linearly (173.0°) while NO is significantly bent (147.6°). The average (160.3°) of the two values is very close to the average experimental values (160.8°). Of importance, the calculated Ru−N-O angle is close to that calculated for X = NCH.

(29) Maseras, F.; Morokuma, K. *J. Comput. Chem.* **1995**, *9*, 1170.

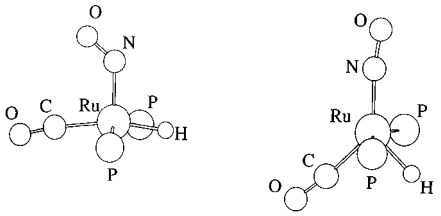

Figure 8. Becke 3LYP optimized structures of $RuH(CO)(NO)(PH_3)_2$, showing SP (left) and TBP forms.

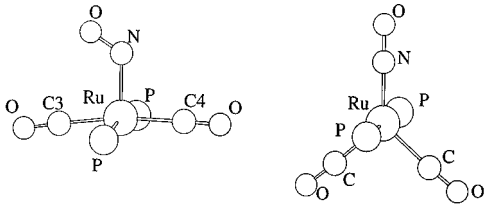

Figure 9. Becke 3LYP optimized structures of $Ru(CO)_2(NO)(PH_3)_2^+$, showing SP (left) and TBP forms.

The barrier to inversion at Ru was calculated. The transition state (C_{2v} symmetry) was located as a square-planar ML_4 complex with linear NO. It is found to be 13.3 kcal·mol^{-1} above the minimum, compatible with the experimentally-determined 19 kcal·mol^{-1}; the latter contains a contribution from solvation and ion pairing.

$RuH(CO)(NO)(PH_3)_2$. Two essentially isoenergetic minima (Table 7; Figure 8) of C_s symmetry are located on the PES. One of them is an SP very similar to the previous ones. The Ru−N−O angle is 129.3°, and NO is bent toward CO. The other minimum is a TBP with axial phosphines, with almost linear NO (171.6°), which bends slightly toward CO. This last bend is very close to the 174.2° experimental value.

$[Ru(CO)_2(NO)(PH_3)_2]^+$. Two isomeric minima (Figure 9), 1.26 kcal·mol^{-1} apart, are located.[28] The more stable SP structure has a bent (121.8°) NO tilted toward the larger N−Ru−C angle. The other minimum is a C_{2v} symmetric TBP with a linear equatorial NO ligand and axial phosphines. The angles within the equatorial plane are distorted with respect to an ideal TBP situation. The N−Ru−C angle (130.3°) is significantly larger than that between the CO ligands (99.4°).

Discussion

Comparison of the ν(CO) value of $Ru(CO)(NO)L_2^+$, 1966 cm^{-1}, with the average ν(CO) of $Ru(CO)_2L_2$ (1902 and 1831 cm^{-1} give a mean of 1867 cm^{-1}) shows the dramatic reduction of back bonding to CO when CO is replaced by isoelectronic NO^+. Alternatively, this can be thought of as the result of adding one proton to the nucleus of carbon in $Ru(CO)_2L_2$. By the criterion of either the E−Ru−C (E = C or N) or the P−Ru−P angles, $Ru(CO)(NO)L_2^+$ is more nonplanar. Since it is π-acid ligand character that causes the distortion from the planarity typical of MX_2L_2 d^8 complexes, the greater nonplanarity of the nitrosyl correlates with greater back donation than in $Ru(CO)_2L_2$. The result of the more potent back bonding to NO^+ is to leave the metal less π-basic (electron rich) in the cationic nitrosyl than in $Ru(CO)_2L_2$. Reactivity toward π-acids or oxidants is thus diminished. This explains why $Ru(NO)(CO)L_2^+$ does not react with H_2 (1 atm) even at −80 °C in toluene. The reaction with CO depends very much on the anion available: $Ru(CO)_2(NO)L_2^+$ with $BAr^F{}_4^-$ anion retains CO strongly and completely, even under vacuum, while BF_4^- anion replaces one CO in $Ru(CO)_2(NO)L_2^+$ under vacuum at 25 °C. In contrast, $RuCl(CO)(NO)L_2$ shows no change (IR and NMR) under CO in toluene.

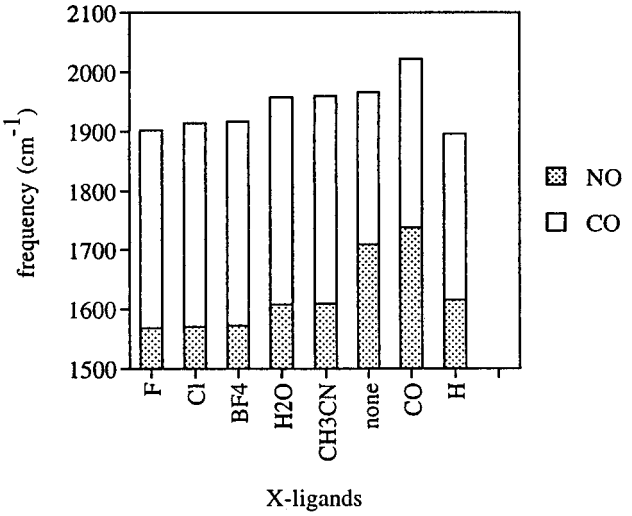

Figure 10. The effect of X ligands on the ν(NO) and ν(CO) values in $RuX(CO)(NO)(P^tBu_2Me)_2$.

Examination of the vibrational frequencies in Figure 10 shows a monotonic increase up to the case X = CO. We argue that this implies analogous structure (square-pyramidal and bent NO) until X = CO, where a trigonal bipyramid with linear NO is adopted. The greater π-acid behavior by linear (*vis-à-vis* bent) NO thus dramatically raises ν(CO). The case where X = H is clearly established in this way as trigonal bipyramidal with linear NO. The reason for this is the strong σ-donor effect of hydride,[30] inducing the Ru^{II} (bent NO^-)-to-Ru^0 (linear NO^+) intramolecular redox change. Note, however, cases where ν(NO) fails to correlate with the expected donor ability of R in $CpM(NO)R_2$ complexes.[31]

In agreement with simple molecular orbital arguments and electron count, the two minima which have been located correspond to a metal in a square-pyramidal or trigonal-bipyramidal geometry.[32] The trigonal bipyramid is significantly distorted from the ideal situation with 120° angles in the equatorial plane. Nevertheless, there is no ambiguity for assigning the structures. For X = Cl, BF_4^-, and HCN, the bond angles between the Ru−N(O) axial bond and the four equatorial Ru−ligand bonds are similar with values between 95 and 100° (Table 7 shows the N−Ru−C angle). In the trigonal-bipyramidal structure, the angle between RuN(O) and the four ligands clearly divides into two families: ∠N−Ru−P approximately 90° and ∠N−Ru−C or X larger than 115°.

Table 7 summarizes the energy pattern associated with the SP and TBP structures. Also given are the experimental ν_{NO} frequencies. The difference in energy between SP and TBP follows closely the variation in NO frequencies: a low ν(NO) corresponds to TBP being high energy or not a minimum. The lowest NO frequency corresponds to a situation where only an SP structure exists. As NO frequency increases, the TBP appears as a competing minimum closer to SP. Absolute energies are not perfect, and it appears that (judging by the case X = H^-) the SP structure is systematically too stable in our study. The crossing of electronic states (d^6 *vs* d^8) associated with the change of NO binding (bent/linear) and metal coordination geometries (TBP/SP) is a challenge for *ab initio* methods. The proper reproduction of the trend at this level of calculations should be viewed as a success for single-determinant methods like Becke3LYP. There is no doubt that

(30) Heyn, R. H.; MacGregor, S. A.; Nadasdi, T. T.; Ogasawara, M.; Eisenstein, O.; Caulton, K. G. *Inorg. Chim. Acta* **1997**, *259*, 5.
(31) Tagge, C. D.; Bergman, R. G. *J. Am. Chem. Soc.* **1996**, *118*, 6908.
(32) Rossi, A. R.; Hoffmann, R. *Inorg. Chem.* **1975**, *14*, 365.

both experimental and theoretical results show that X = F^- and Cl^- favors the SP structure and X = H^- and CO favor the TBP structure. The assignment is more difficult for X = H_2O and CH_3CN. The experimental results are in favor of a TBP structure. The CO frequencies (Figure 10) are a reliable indicator for this change of structure since there is a significant increase of ν_{CO} going from SP to TBP; this is clearly not caused by the oxidation state *reduction*, but instead by the dominant π-acidity of linear NO^+. From the theoretical point of view, the difference of 5 kcal·mol^{-1} could be reversed at higher levels of calculation. We thus conclude that these calculations systematically underestimate the stability of the TBP by 5−6 kcal·mol^{-1}, based on the error calculated for X = H^-. Therefore, each time a TBP structure is located, it is a viable candidate as the most stable isomer.

The study of the competition between bent and linear NO reveals a complex situation. For Cl^- and BF_4^-, the NO ligand is strongly bent and the angle is close to that reported in numerous complexes which are commonly accepted to contain bent NO. For X = CO and H^-, the NO is clearly linear and the metal coordination polyhedron is changed to TBP. In agreement with the calculations, the NO frequencies are the lowest (around 1570 cm^{-1}) for X = F^-, Cl^-, and the highest for X = CO (1738 cm^{-1}). The cases for RCN and for the X ligand absent are especially interesting. An angle of 150 ± 4° is too far from the two extremes (bent or linear) to be identified with either of them. The experimental ν_{NO} frequency is also well separated from the two limiting frequencies. In the case of no ligand, the significant bend of the NO indicates that Ru(0) is a powerful electron donor and NO a powerful π acceptor. In the case of $Ru(CO)_2(PR_3)_2$, the Ru−C−O angle was found to be 168°. The difference in angle between CO and NO parallels their ranking of π-accepting ability.[33] The weakly bonded ligands like RCN and H_2O lead to situations similar to the no-ligand case. In these systems, should NO be viewed as NO^+ or NO^-? Limiting the subtle change in NO geometry to a binary choice is unrealistic. Enemark and Feltham[6] have anticipated this situation, phrased there (Figure 15 of ref 6) in terms of near degeneracy of metal d-orbitals and totally π-antibonding M−N−O orbitals; in such cases, they state the inadequacy of limiting NO^+ and NO^- labels. We also advocate here a preference for non-integer oxidation states. Such situations exist in all organometallic−inorganic systems, but very few ligands are able to show *geometrical changes* diagnostic of small (non-integral) changes in metal oxidation states. The NO ligand is thus especially informative for this purpose.[34]

What are the factors which favor the SP or the TBP? It should be noted that the structures with a clear preference for a single SP structure correspond to X with π-donor capability. No clear MO pictures can rationalize this structure. However, of great interest is the fact that 16-electron (SP) species have been characterized as strongly persistent for $RuX(H)(CO)(PH_3)_2$ when X is a π donor such as F, Cl, or OR.[30] This preference for bent NO for π donors X may be the most significant proof that π donors stabilize electron-deficient complexes.

Acknowledgment. This work was supported by the U.S. National Science Foundation. The international collaboration was supported by an NSF and CNRS (PICS) agreement for US/France collaboration. We thank Johnson Matthey/Aesar for material support. F.M. thanks CNRS for a research associate position and N.G.P.'s work was supported by the EEC network CHRXCT 93.0152.

Supporting Information Available: Full crystallographic details and structural parameters from the *ab initio* calculations (15 pages). See any current masthead page for ordering and Internet access instructions.

JA970563J

(33) The electron transfer from Ru to CO in $Ru(CO)_2(PR_3)_2$ seems therefore to be also a factor in the CO bending of this species, in addition to the interactions previously discussed. See ref 1a.

(34) Marinelli, G.; Streib, W. E.; Huffman, J. C.; Gagné, M. R.; Takats, J.; Dartiguenave, M.; Chardon, C.; Jackson, S. A.; Eisenstein, O.; Caulton, K. G. *Polyhedron* **1990**, *9*, 1867.